

Intermolecular Electron Transfer Reactivity Determined from Cross-Rate Studies

STEPHEN F. NELSEN^{*,†} AND
JACK R. PLADZIEWICZ^{*,‡}

Department of Chemistry, University of Wisconsin–Madison, Wisconsin 53706-1396, and Department of Chemistry, University of Wisconsin–Eau Claire, Wisconsin 54702-4004

Received August 10, 2001 (Revised Manuscript Received January 21, 2002)

ABSTRACT

Electron-transfer cross-reactions between neutral molecules and their radical cations spanning a wide range of structural type and intrinsic reactivity have been analyzed using classical Marcus theory. The principal factor found to govern intrinsic reactivity is the inner-shell bond reorganization energy. The HOMO–LUMO overlap of alkyl groups on reacting molecules is generally sufficient to provide facile electron transfer; however, a significant steric effect on this overlap is observed for hydrazines with alkyl groups larger than methyl.

Introduction

Relationships between structure and reactivity form the core of our understanding of chemistry and are fundamental in allowing prediction of which compounds to employ for various functions. A basic determining factor of reactivity is the driving force for a reaction, ΔG^0 . Most structural changes alter both the driving force and intrinsic reactivity—the reactivity at constant driving force. Especially well-studied series that cover very large ranges in reactivity include solvolyses in polar solvents and acid-catalyzed hydration of alkenes.¹ Detailed interpretation of most of these reactions is limited, because the free energy change associated with the elementary steps is not known. Marcus pointed out that the natural comparison point for intrinsic reactivity for electron transfer (ET) reactions is the self-exchange-ET rate constant, k_{ii} .² He described the relationship between intrinsic reactivity and the rate constant for outer-sphere electron transfer for a net chemical reaction, k_{12} . For a reaction between a neutral species, i^0 , and a different radical cation, j^+ , eq 1,



electrostatic factors are unimportant, and the relationship is astonishingly simple, eq 2.²

$$k_{ij}(\text{calcd}) = (k_{ii}k_{jj}K_{ij}f_{ij})^{1/2} \quad (2a)$$

$$\ln(f_{ij}) = [\ln(K_{ij})^2 / [4 \ln(k_{ii}k_{jj}/Z^2)]] \quad (2b)$$

The self-exchange rate constants k_{ii} and k_{jj} , and the equilibrium constant, K_{ij} , are the principal parameters determining k_{ij} . A preexponential factor, Z , of $10^{11} \text{ M}^{-1} \text{ s}^{-1}$ is often used; for our systems, the results are relatively insensitive to the value employed. The f_{ij} is 1 when $K_{ij} = 1$ and decreases as the reaction becomes more exoenergetic; no reactions in our data set have f_{ij} less than 0.1. Formal potentials were determined using CV for all couples described here, and the K_{ij} 's used in eq 2 are derived from them. A more general form of eq 2 that includes the work terms necessary for multiply charged reactants, has been successfully applied to a wide variety of inorganic, organic, organometallic, and biochemical reactions.^{3–5} However, studying couples having similar k_{ii} values principally tests the dependence of k_{ij} upon K_{ij} , which is known to work well.^{3–5}

This work describes our results for a database of ET reactions, such as those described in eq 1, among a large set of compounds diverse in both intrinsic reactivity and structure, from which we have extracted reliable estimates of the intrinsic ET reactivity of all compounds in the set. The database allows an unprecedented test of structure–reactivity relationships and modern ET theory with some unexpected results, including close agreement with classical Marcus theory, striking steric effects, and estimates of the ET overlap integral and its dependence on reactant type and structure.

Determination of ΔG_{ii}^\ddagger (fit) Values. We have measured k_{ij} using stopped-flow spectrophotometry for a diverse group of 0/1+ couples for which $E^{0'}$ has been measured under the same conditions. Our principal contribution has been to include couples having a very large range of k_{ii} values. This has been achieved especially by including hydrazines of varied structural types, which causes a wide variation in the size of the geometry change between the oxidation states and, hence, the reorganization energy.^{6–11} Having both large and small k_{ii} couples available for study greatly expands the range of accessible compounds, as compared to those that can be studied directly under self-exchange-ET conditions. The reaction is always at equilibrium under self-exchange-ET conditions, and electron exchange is usually detected using magnetic resonance (MR) line-broadening. However, the amount of broadening becomes too small to measure accurately for k_{ii} below $\sim 7 \times 10^2 \text{ M}^{-1} \text{ s}^{-1}$.¹² The upper limit for self-exchange-ET studies appears to be $\sim 3 \times 10^9 \text{ M}^{-1} \text{ s}^{-1}$ (that for tetra-

Stephen Nelsen is a professor at the University of Wisconsin–Madison. He received his BS degree at the University of Michigan, Ann Arbor, and his Ph.D. at Harvard University, working with P. D. Bartlett. His research interests are in physical organic chemistry, and include free radical, radical ion, and electron-transfer reactions; lone-pair effects and σ , π interaction effects on reactivity; and the preparation of theoretically significant molecules.

Jack Pladzewicz is a professor and the department chair at the University of Wisconsin–Eau Claire. He received his BS degree at the University of Wisconsin–Eau Claire; Ph.D. at Iowa State University, working with James H. Espenson; and did postdoctoral work at Stanford University, working with Henry Taube and E. E. van Tamelen. His research interests include stereoselective metalloprotein electron transfer and activation of small molecules to single electron transfer.

* Correspondence may be addressed to either author.

† University of Wisconsin–Madison.

‡ University of Wisconsin–Eau Claire.

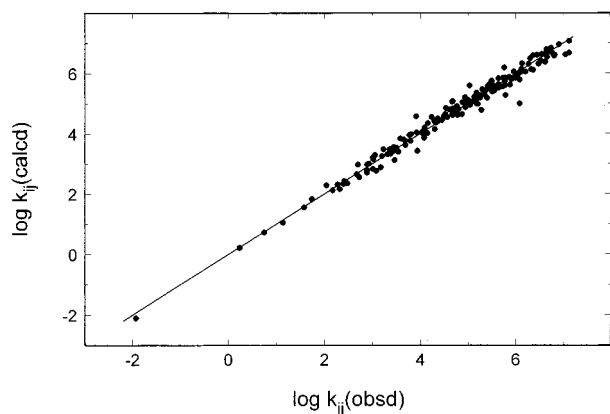


FIGURE 1. Plot of $\log k_{ij}(\text{calcd})$ versus $\log k_{ij}(\text{obsd})$ for the 164-reaction data set.

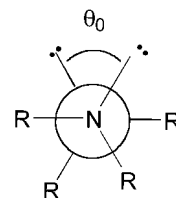
methyl-*p*-phenylenediamine, $\text{TMPD}^{0/+}$).¹³ Nearly two-thirds of the couples we have studied by stopped-flow (36 of 56) could not have their k_{ii} values measured under direct self-exchange conditions.

Stopped-flow kinetic data has frequently been used to establish relative reactivity by selecting a few isolable “oxidants” and determining the k_{ij} for their reactions with several reduced species. Extracting the k_{ii} for some compounds then required directly measuring k_{ii} for the others, typically using MR methods. In contrast, we do not use any directly measured self-exchange rate constants to extract k_{ii} from our k_{ij} data. Instead, the $k_{ij}(\text{obsd})$ and E° values, both measured at 25 °C in acetonitrile containing 0.1 M tetrabutylammonium perchlorate, are subjected to a least-squares fit of all of the data to eq 2 to extract $k_{ii}(\text{fit})$ values.^{9–11} The observed k_{ij} values are fit well using eq 2, as shown graphically in Figure 1. One hundred and fifty of the calculated k_{ij} values (92%) lie within a factor of 2 of the experimental value using the $k_{ii}(\text{fit})$ s for the calculation, and an additional eight (5%) are within a factor of 3. Using eq 2 to obtain reliable $k_{ii}(\text{fit})$ s requires measuring k_{ij} values between a wide range of the couples, which we have done.^{9–11} The range of $k_{ij}(\text{fit})$ values obtained is very large, 2×10^{14} , but we have found no dependence of the scatter of the $k_{ij}(\text{fit})$ s on intrinsic reactivity, ΔG° , or type of reaction partner.

The $k_{ii}(\text{fit})$ values have been converted to Eyring $\Delta G_{ii}^{\ddagger}(\text{fit})$ values to allow their linear comparison, and we shall refer to these $\Delta G_{ii}^{\ddagger}(\text{fit})$ values as intrinsic reactivity. For all of the reactions that we have been able to study, eq 2 works very well. Compounds of similar structure have similar intrinsic reactivity, and individual $\Delta G_{ii}^{\ddagger}(\text{fit})$ established from a few reactions do not change much as more reactions are studied, suggesting that $\Delta G_{ii}^{\ddagger}(\text{fit})$ is, indeed, determined to a reliability of a few tenths of a kcal/mol (the average $\Delta \Delta G_{ii}^{\ddagger}(\text{fit}) = |0.592 \ln [k_{ij}(\text{obs})/k_{ij}(\text{fit})]|$ for the entire data set is 0.19 kcal/mol). Consequently, we believe they are useful for understanding the relationship between structure and reactivity. Moreover, there is a good agreement between $\Delta G_{ii}^{\ddagger}(\text{fit})$ and directly measured self-exchange activation energy, $\Delta G_{ii}^{\ddagger}(\text{self})$ for the 11 couples for which both have been determined, but the $\Delta G_{ii}^{\ddagger}(\text{fit})$ values are systematically slightly larger than the $\Delta G_{ii}^{\ddagger}(\text{self})$

values, and the average $\Delta \Delta G_{ii}^{\ddagger} = \Delta G_{ii}^{\ddagger}(\text{fit}) - \Delta G_{ii}^{\ddagger}(\text{self}) = 0.6 \text{ kcal mol}^{-1}$.^{9,10} The $\Delta G_{ii}^{\ddagger}(\text{fit})$ values arise from experimental rate constants for cross-reactions, so they must include the effect of averaging the preexponential factors for the cross-reactions studied, but $\Delta G_{ii}^{\ddagger}(\text{self})$ values depend only on the preexponential factor for the self-exchange-reaction, and we believe that this may be the origin of this small difference. $\text{TMPD}^{0/+}$ is the lowest barrier and least sterically encumbered couple for which both values are available^{13b,c} and has the largest $\Delta \Delta G_{ii}^{\ddagger}$, 1.5 kcal mol⁻¹. The $\Delta G_{ii}^{\ddagger}(\text{fit})$ value for $\text{TMPD}^{0/+}$ was determined from reactions with eight hydrazines: six tetra- α -branched, 22/*t*BuMe and 33NNMe₂. None of the cross reactions is likely to have as good an orbital overlap between the reaction partners at the transition state as can TMPD^0 with TMPD^+ , and this might be the principal factor causing $k_{ii}(\text{self})$ to be 13-fold larger than $k_{ii}(\text{fit})$. At the other reactivity extreme for which both barriers are available, the very hindered couple $\text{iPr}_2\text{N})_2^{0/+}$ has a $\Delta \Delta G_{ii}^{\ddagger}$ within experimental error of zero.

Factors Determining $\Delta G_{ii}^{\ddagger}(\text{fit})$ Values. Thirty-two hydrazine couples spanning a very large range of intrinsic reactivity, 16.5 kcal mol⁻¹ or 84% of the total $\Delta G_{ii}^{\ddagger}(\text{fit})$ range observed, are listed in approximately descending order of their $\Delta G_{ii}^{\ddagger}(\text{fit})$ in Table 1.¹⁴ Abbreviations are used for the structures, and examples for the cyclic compounds are shown in Chart 1. A u indicates unsaturation β, β' to the hydrazine nitrogens, and k is used for a 3-oxo group in a 33N bicyclic ring. The ET reactivity of hydrazines falls into five groups on the basis of the connectivity of their substituents. The reason for this is that the lone-pair–

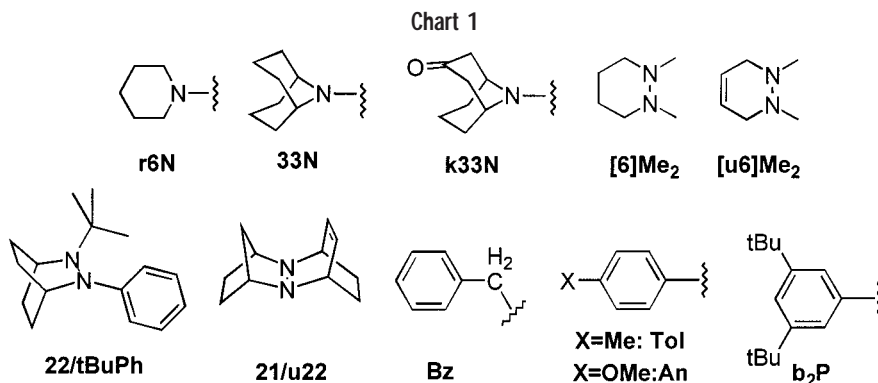


lone-pair twist angle about the NN bond of the neutral form, θ_0 , depends on the connectivity of the substituents. θ_0 is a primary structural feature influencing intrinsic reactivity, because it strongly affects the reorganization energy. Neutral hydrazines have significantly pyramidalized nitrogens¹⁴ and electronically prefer $\theta_0 \sim 90^\circ$ conformations, because this allows maximum lone pair, σ^* stabilizing interactions (often stated as avoiding overlap of the lone pair orbitals). The θ_0 values for the hydrazines were determined using photoelectron spectroscopic lone pair–lone pair orbital vertical ionization potential differences¹⁵ and, in several cases, by X-ray crystallography.¹⁶ Hydrazine radical cations have one antibonding (π^*) and two bonding (π) electrons and, therefore, have geometries that are very different from their related neutral molecules, showing a strong electronic preference for being untwisted (θ_+ near 0 or 180°), and their nitrogens are considerably flattened (0 and 180° twists become the same when the nitrogens become planar).¹⁴ The largest geometry changes and, hence, the largest reorganization energies and ET

Table 1. Intrinsic Reactivity, NN Twist Angle Groups, Estimated ΔG_{ii}^* Values, and Calculated Vertical Reorganization Enthalpies of Hydrazines^a

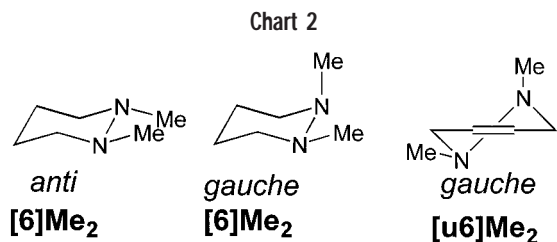
no.	couple	$\Delta G_{ii}^{\ddagger}(\text{fit})$	group (θ_0)	H_{ab} , ΔG_{ii}^* pairs	ΔH_v
1	nPr ₂ N) ₂ ^{0/+}	21.9	1($\theta_0 \sim 90^\circ$)	[0.01] 17.1	
2	Et ₂ N) ₂ ^{0/+}	21.8	1	[0.01] 17.0	14.0 ^b
3	nHx ₂ N) ₂ ^{0/+}	21.4	1	[0.01] 16.6	
4	Bz ₂ N) ₂ ^{0/+}	21.1	1	[0.01] 16.3	13.5
5	iPrMeN) ₂ ^{0/+}	20.2	1	0.026 ← [16.6]	
6	iPr ₂ NNMe ₂ ^{0/+}	20.7	1	0.018 ← [16.6]	
7	iPr ₂ N) ₂ ^{0/+}	21.0	1 ^c	[0.01] 16.2	13.9
8	cHx ₂ N) ₂ ^{0/+}	19.6	1 ^c	[0.01] 14.8	
9	nPr ₂ NNMe ₂ ^{0/+}	19.4	1	0.08 ← [17.0]	
10	nPrMeN) ₂ ^{0/+}	19.4	1	0.08 ← [17.0]	
11	nBuMeN) ₂ ^{0/+}	19.3	1	0.08 ← [17.0]	
12	r7NNMe ₂ ^{0/+}	18.2	1	0.21 ← [17.0]	
13	Me ₂ N) ₂ ^{0/+}	17.3	1	0.45 ← [17.0]	15.1
14	r6NNMe ₂ ^{0/+}	16.8	1	[0.45]16.5	13.7
15	r5NNMe ₂ ^{0/+}	16.7	1	[0.45]16.4	14.7
16	k33N) ₂ ^{0/+}	15.2	2 ^c ($\theta_0 = 180^\circ$)	0.002 ← [8.9]	
17	k33NN33 ^{0/+}	14.2	2	0.006 ← [8.9]	
18	33N) ₂ ^{0/+}	13.5	2 ^c	[0.01] 8.9	9.1 ^d
19	21/Me ₂ ^{0/+}	16.1	3($\theta_0 \sim 120^\circ$)		
20	22/tBuPr ^{0/+}	15.8	3	[0.001] 11.1	10.5
21	22/tBuMe ^{0/+}	15.2	3		11.6
22	[u6]Me ₂ ^{0/+}	17.4	only <i>gauche</i>		
23	[6]Me ₂ ^{0/+}	15.0	<i>anti</i> > <i>gauche</i>		
24	22/22 ^{0/+}	14.7	4 ^c ($\theta_0 \sim 0^\circ$)	[0.01] 10.0	8.3 ^e
25	21/u22 ^{0/+}	13.4	4	[0.01] 8.8	9.7
26	22/u22 ^{0/+}	13.2	4 ^c	[0.01] 8.6	9.1
27	22/u23 ^{0/+}	12.8	4 ^c	[0.01] 8.2	9.6
28	21/21 ^{0/+}	12.7	4	[0.01] 8.1	8.8
29	22/tBuPh ^{0/+}	13.3	5 ^c (<i>n</i> -aryl)		9.5
30	22/Ph ₂ ^{0/+}	11.0	5		9.0
31	(b ₂ P) ₂ N) ₂ ^{0/+}	8.2 ^f	5		
32	tol ₂ N) ₂ ^{0/+}	5.4	5		

^a $\Delta G_{ii}^{\ddagger}(\text{fit})$, ΔG_{ii}^* , and ΔH_v in kcal mol⁻¹; ΔH_v calculated using AM1. ^b This entry corresponds to using the minimum enthalpy neutral and cation conformations obtained. Values for various minimums of neutral and cation in other combinations range from 13.2 to 14.8 kcal mol⁻¹. Obtaining such ranges is an increasing problem as conformational complexity increases. ^c Crystal structures available. ^d Constrained to $\theta = 180^\circ$; a larger value is obtained using the AM1 optimum θ values (which deviate from the experimental values of 180°). ^e AM1 twist angle for the neutral is 0° , which is incorrect (it is really about 15°), making this value too small relative to the other Group 4 entries. ^f Three of the reactions studied have $k_{ii}(\text{fit})/k_{ii}(\text{obs})$ values lying outside the range 3 or 0.33 (so one-half of the six reactions studied that fit eq 2 poorest involve this couple). The structure of this compound was given incorrectly in ref 11.



barriers ($\Delta G_{ii}^{\ddagger}(\text{fit}) \geq 16.7$ kcal mol⁻¹) occur for Group 1, $\theta_0 = \sim 90^\circ$, hydrazines, entries 1–15 (e.1–15) of Table 1. Group 2, $\theta_0 = 180^\circ$, compounds (e.16–18) result when the substituents at nitrogen become large enough and also are unable to rotate away from N–C_α twist angles that give large nonbonded steric interactions between α -substituents. Just having four α -branched substituents, as for iPr₂N)₂ (e.7) and *c*-Hx₂N)₂ (e.8), is not sufficient to make $\theta_0 = 180^\circ$ conformations predominate, because their alkyl groups can rotate out of conformations having large steric interactions with substituents on the other nitrogen. The Group 3 hydrazines (e.19–21) are forced to $\theta_0 \sim 120^\circ$,

because they have near- 0° bicyclic ring CNNC angles imposed by their structures. The electronically least favorable $\theta_0 \sim 0^\circ$ conformations are formally possible if the alkyl groups are syn to each other, but a syn conformation has never been observed in a bicyclic hydrazine. In contrast, the chair ring of dimethylhexahydropyridazine, [6]Me₂, allows both *anti* ($\theta_0 \sim 180^\circ$) and *gauche* ($\theta_0 \sim 60^\circ$) conformations to be occupied (Chart 2); they differ in energy by only 0.2 kcal mol⁻¹.¹⁷ The intrinsic reactivity for [6]Me₂^{0/+} is slightly less than that of the $\theta_0 \sim 180^\circ$ 33N)₂^{0/+}, which also has flatter nitrogens because of its α -branched carbons. Despite differing in structure

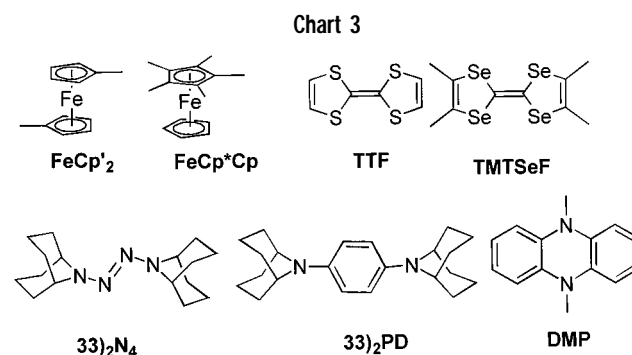


by only two hydrogens, dimethyltetrahydro-pyridazine [u6]Me₂ can be detected in only the gauche conformation¹⁷ and we argue, as a result, has reactivity close to that of the unhindered Group 1 hydrazine Me₂N₂. Group 4 hydrazines have both CNNC angles forced to be near 0°, which produces syn lone pair neutral conformations having $\theta_0 \sim 0^\circ$, and nonbonded steric interactions flatten their nitrogens relative to the $\theta_0 = 180^\circ$ Group 2 ones. Group 4 hydrazines, therefore, have especially small geometry changes upon electron loss and are the lowest $\Delta G_{ii}^{\ddagger}(\text{fit})$ hydrazines that lack aryl substitution, and their ET could be studied by direct self-exchange methods as well as stopped-flow.^{12,18} The highest barrier couple of this group is 22/22, shown by crystallography to be twisted 15° in the neutral form.^{16b} A twisted neutral structure increases the vertical reorganization energy, λ_v , because twisting the cation radical is difficult. The other saturated compounds are untwisted, in agreement with calculated geometries, and have their $\Delta G_{ii}^{\ddagger}(\text{fit})$ values in the order of their calculated λ_v values for electron loss.¹⁸ Decreasing ring size makes the nitrogens more pyramidal in both oxidation states, and the nitrogens are pyramidal enough for 21/21⁺ that the barrier to their becoming planar is 4.6 kcal mol⁻¹, measured by ESR.¹⁹ Successively replacing alkyl substituents by aryl ones (Group 5) substantially lowers the ET barrier. For example, replacing the isopropyl of 22/tBu-iPr (e.20) by phenyl to give 22/tBuPh, (e.29) lowers $\Delta G_{ii}^{\ddagger}(\text{fit})$ by 2.5 kcal mol⁻¹, and a second aryl substitution in going to 22/Ph₂ (e.30) lowers $\Delta G_{ii}^{\ddagger}(\text{fit})$ an additional 2.3 kcal mol⁻¹. The tetra-arylhydrazines, e.31 and e.32, are the most reactive hydrazines studied. The $\Delta G_{ii}^{\ddagger}(\text{fit})$ for tol₂N₂ (e.32) lies between those for the unhindered nearly planar aminoaromatic couples, TMPD and DMP. Turning to nonhydrazine couples in Table 2 and Chart 3, the bicyclononyl protected 2-tetrazenes, (33)₂N₄ (e.33) and (33)₂-PD (e.34), are intermediate in reactivity between hydrazines and aromatic compounds. They are much more reactive than their hydrazine counterparts: $\Delta \Delta G_{ii}^{\ddagger}(\text{fit}) = 3.7$ kcal mol⁻¹ for the 33N-substituted systems (e.18 and e.34) and 4.5 kcal mol⁻¹ for the keto systems (e.16 and e.33). The four ferrocenes, e.35–38, lie in a narrow reactivity range and are less reactive than any of the aromatic organic compounds. Aromatic compounds make up the upper quartile of ET reactivity measured. The $k_{ii}(\text{fit})$ values for the fastest ones are near or at the diffusion limit: TMTSF^{0/+}, 1.2×10^{11} ; An₃N^{0/+}, 2.4×10^{10} ; and TTF^{0/+}, 1.4×10^{10} M⁻¹ s⁻¹ (e.46–44); so their intrinsic reactivity can be accurately determined only by using cross-reactions. The $k_{ii}(\text{fit})$ obtained for An₄PD^{0/+} (e.42), 3.6×10^8 M⁻¹ s⁻¹, is more than a factor of 100 less than

Table 2. Intrinsic Reactivity for Non-Hydrazine Couples^a

no.	couple	ΔG_{ii}^{\ddagger}	$\Delta G_{ii}^{\ddagger b}$	$(\Delta H_v + 2)^c$	type
33	k33) ₂ N ₄ ^{0/+}	10.7			2-tetrazene
34	33) ₂ N ₄ ^{0/+}	9.8			2-tetrazene
35	FeCp ₂ ^{0/+}	8.3			ferrocene
36	FeCp [*] Cp ^{0/+}	8.0			ferrocene
37	FeCp [*] 2 ^{0/+}	7.9			ferrocene
38	FeCp ₂ ^{0/+}	7.7			ferrocene
39	k33) ₂ PD ^{0/+}	7.2			PD
40	TMPD ^{0/+}	6.5	6.58	6.67	PD
41	33) ₂ PD ^{0/+}	6.2			PD
42	An ₄ PD ^{0/+}	5.8			triarylamine/PD
43	DMP ^{0/+}	5.3	5.43	5.88	aromatic
44	TTF ^{0/+}	3.6	3.83	3.73	aromatic
45	An ₃ N ^{0/+}	3.3			triarylamine
46	TMTSF ^{0/+}	2.3	2.6 ^d		aromatic

^a $\Delta G_{ii}^{\ddagger}(\text{fit})$, ΔG_{ii}^{\ddagger} , and ΔH_v in kcal mol⁻¹. ^b Calculated with $H_{ab} = 0.5$, $K_e = 1$ using eqs 3–5. ^c AM1 calculated, plus 2 kcal mol⁻¹ as an estimate of $\lambda_s/4$. ^d If a 2 kcal mol⁻¹ solvent contribution to ΔG_{ii}^{\ddagger} is assumed, this leaves only 0.6 kcal mol⁻¹ for ΔH_v .



that for An₃N^{0/+} but close to that obtained under self-exchange conditions by NMR in CDCl₃, $3.5(3) \times 10^8$.²²

Electronic Coupling and Reorganization Energy Effects on Intrinsic Reactivity. It is revealing to consider the observed intrinsic reactivity using more modern ET theory. The fundamental assumption giving rise to eq 2 is that the reactions are activation-barrier-limited, so the barrier for the cross-reaction will be the average of those for the related self-exchange reactions.² Marcus obtained eq 2 by assuming that ET reactions are adiabatic, and preexponential factors should be nearly constant for adiabatic reactions. The adiabatic preexponential factor is often approximated as $3 \times 10^{10} h\nu_v$, where $h\nu_v$ is the energy corresponding to the inherent barrier-crossing frequency, usually thought of as a bond-stretching mode. The $h\nu_v$ values for all of the couples studied here are believed to vary between ~ 400 and 1600 cm⁻¹. However, achieving adiabaticity requires rather large H_{ab} values, which are not believed to occur for most intermolecular ET reactions, and certainly not for ones between compounds as hindered as for most of the cross-reactions reported here. In a recent review on ET, Bixon and Jortner said that although there was “lively discussion” in the 1960s about whether ET reactions were adiabatic or nonadiabatic, it has now been established that the great majority are nonadiabatic.²¹ But if this were the case for our reactions, eq 2 would not work well, because nonadiabatic reaction rate constants are not only controlled by activation barriers (or Franck–Condon factors using

Jortner's vibronic coupling theory) but also by widely varying preexponential factors. The nonadiabatic preexponential factor is proportional to the ET orbital overlap integral squared, $(H_{ab})^2$ and is also directly proportional to e^{-S} , where S is the vibronic coupling constant (Huang–Rhys factor), which is the ratio of $h\nu_v$ to the internal vibrational component of λ , λ_v . Tetraalkylhydrazines have unusually large S values, exceeding 20, but aromatic compounds and ferrocenes have much smaller S values, certainly under 6, so simply from the e^{-S} term, a factor of above a million-fold faster ET should occur for aromatic compounds and ferrocenes than for hydrazines. The consequences of such an effect on the preexponential term are not observed experimentally. The same k_{ii} value suffices to calculate k_{ij} whether a hydrazine couple is reacted with a ferrocene, an aromatic compound, or another hydrazine. Equation 2 would not fit our data so well if the preexponential factor were sensitive to S .

To interpret our data, we modify the simplest non-adiabatic rate equation of Levich and Dogonadze.²¹ The modifications are (a) the ET activation free energy, ΔG^* , of classical Marcus–Hush two-state theory (eq 3)³ replaces $\lambda/4$ to allow reactions that do not have vanishingly small H_{ab} to be treated

$$\Delta G^* = \lambda/4 - H_{ab} + (H_{ab})^2/\lambda \quad (3)$$

and (b) the encounter complex formation constant, K_e , has been inserted so that the equation can be used for intermolecular ET. This results in eq 4, which like adiabatic Marcus theory, uses only λ and H_{ab} to predict the rate constant.

$$k_{L\&D}(25\text{ }^\circ\text{C}) = (1.52 \times 10^{14})(K_e H_{ab}^2/\lambda^{1/2}) \exp[-\Delta G^*/RT] \quad (4)$$

Importantly, it is necessary to know both H_{ab} and K_e to extract ΔG^* (and λ) from intrinsic reactivity. There is, however, no way of experimentally determining K_e for our reactions, and factors that raise H_{ab} appear likely to raise K_e , as well. Interpretation of intermolecular reactions must include both factors, so we shall use $H'_{ab} = K_e^{1/2} H_{ab}$ (units, $M^{-1/2}$ kcal mol⁻¹) in discussing our results.¹¹ Substitution of $k_{ij}(\text{fit})$ for $k_{L\&D}(25\text{ }^\circ\text{C})$ in eq 4 leads to eq 5.

$$\Delta G^*_{ii} = 0.592[32.655 - \ln(k_{ij}(\text{fit})) + \ln(H'_{ab})^2/\lambda^{1/2}] \quad (5)$$

We believe that eqs 3–5 provide an internally consistent interpretation of our data and allow important conclusions to be drawn about the reactions studied.

Figure 2 shows an example of the dependence of $\lambda/4$ and ΔG^*_{ii} on H'_{ab} . The shape of the curve is similar to that obtained using an adiabatic rate equation with an electronic transmission coefficient in the preexponential term, but using eq 4 requires fewer parameters, because one does not need to know the $h\nu_v$ and λ_v to calculate the preexponential term.¹¹ All of the points on the solid line of Figure 2 correspond to the same $\Delta G^*_{ii}(\text{fit})$ value, emphasizing that if intrinsic reactivity correlates with λ , H'_{ab} cannot be changing very much. The curved lines of

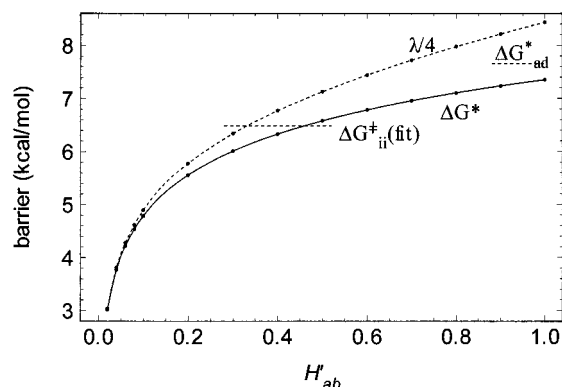


FIGURE 2. Plot of ΔG^* (using eqs 3–5) and the corresponding $\lambda/4$ (using eq 3 with H_{ab} replaced by H'_{ab}) for the $k_{ij}(\text{fit})$ of $\text{TMPD}^{0/+}$ ($\Delta G^*_{ii}(\text{fit}) = 6.5$ kcal/mol). An $h\nu_v$ of 1500 cm^{-1} was used to calculate ΔG^*_{ad} .

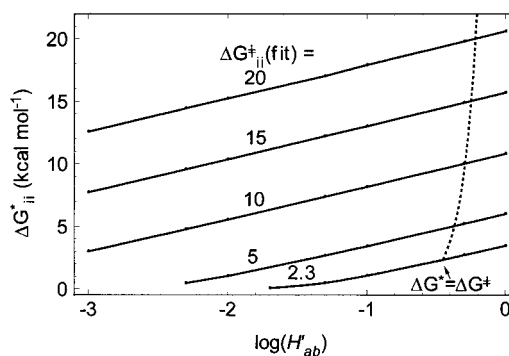


FIGURE 3. Plots of ΔG^*_{ii} versus $\log(H'_{ab})$ for various values of $\Delta G^*_{ii}(\text{fit})$.

Figure 2 become nearly linear when $\log(H'_{ab})$ is used as the x axis, as shown in Figure 3, and the lines for various $\Delta G^*_{ii}(\text{fit})$ values are displaced by approximately the difference in $\Delta G^*_{ii}(\text{fit})$. The broken line in Figure 3 shows $\log(H'_{ab})$ values for which ΔG^*_{ii} is equal to $\Delta G^*_{ii}(\text{fit})$ according to eq 5, dropping from about $H_{ab} = 0.63$ for the largest $\Delta G^*_{ii}(\text{fit})$ (~ 22 kcal mol⁻¹ for nR₄N₂) to 0.35 for the smallest (2.3 kcal mol⁻¹ for TMTSF). It may be seen that ΔG^*_{ii} is significantly less than $\Delta G^*_{ii}(\text{fit})$ for high-barrier compounds that have small H_{ab} , but for less-hindered compounds that have higher H_{ab} values, mostly the aromatics, ΔG^*_{ii} will approach $\Delta G^*_{ii}(\text{fit})$.

Which H_{ab} values are appropriate for intermolecular ET reactions has not been clear. For what is probably the most discussed example, Grampp and Jaenicke suggest that the $\text{TMPD}^{0/+}$ transition state has a geometry with the aryl rings in π -stacking contact with parallel long axes, as they are in crystals, and that a rather low value of $H_{ab} = 0.1$ kcal mol⁻¹ is necessary to be consistent with the directly measured k_{ij} value,¹³ but Rauhut and Clark have calculated values using ab initio theory for transition states having a wider range of geometries, estimating an H_{ab} of 0.65 kcal mol⁻¹.²² Weaver and co-workers have argued from solvent studies on self-exchange-ET rate constants of metallocenes that ferrocene and decamethylferrocene have H_{ab} values of 0.1 and 0.2 kcal mol⁻¹, respectively.²³ We consider our data on these and related molecules using the ΔG^*_{ii} versus $\log(H'_{ab})$ plot of Figure 4. These are

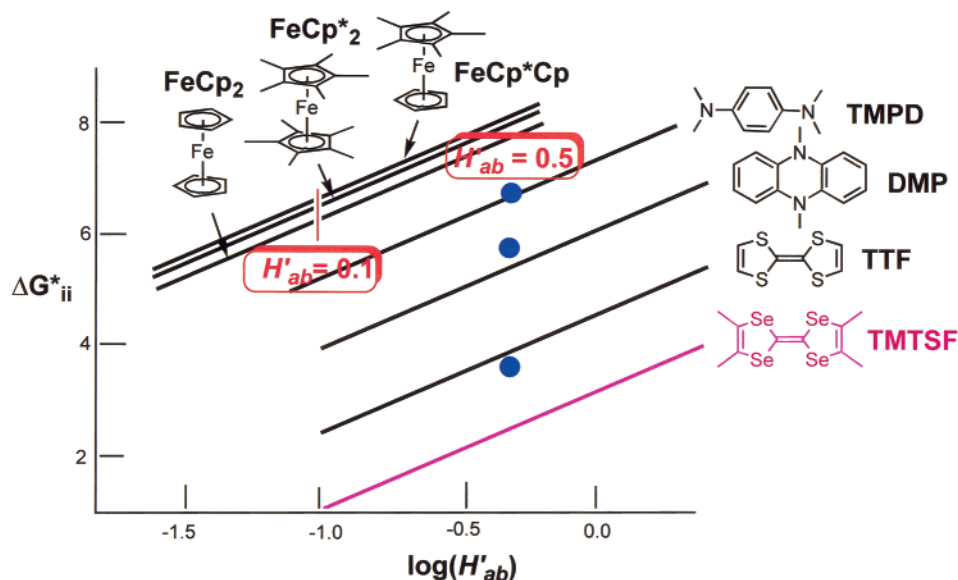


FIGURE 4. Plots of ΔG_{ii}^{\ddagger} versus $\log(H'_{ab})$ for some ferrocene and aromatic couples.

the least-hindered compounds studied, so their H_{ab} values should be the highest. The enthalpy portion of λ_v can be calculated using the AM1 semiempirical method, and rather good correlation between the calculated contribution to the barrier (one-quarter of the calculated internal reorganization enthalpy), which we will call ΔH_v , and $\Delta G_{ii}^{\ddagger}(\text{fit})$ has been noted.^{10,11} In Figure 4, we highlight an H'_{ab} value of 0.5 (x axis value of -0.3) for the planar aromatics, where the ΔH_v values for $\text{TMPD}^{0/+}$, $\text{DMP}^{0/+}$, and $\text{TTF}^{0/+}$ plus 2 kcal mol⁻¹ (equivalent to using $\lambda_s = 8$ kcal mol⁻¹ for these compounds) lie close to the experimental data lines. If the H_{ab} values for these couples differed by much more than a factor of 2 (an increment of 0.3 in the $\log(H_{ab})$ x axis value), one would expect the separations of the ΔG_{ii}^{\ddagger} values to become significantly different from those of the ΔH_v values. Using $H'_{ab} = 0.5$ is also close to using Clark's ab initio calculated H_{ab} value for $\text{TMPD}^{0/+}$ (K_c is estimated to be somewhat less than 1 M⁻¹).¹³ Another reason for choosing $H'_{ab} = 0.5$ as an estimate for these compounds is that the fastest couple studied, $\text{TMTSF}^{0/+}$ (for which ΔH_v is not available using AM1), has a $\Delta G_{ii}^{\ddagger}(\text{fit})$ of only 2.3 kcal mol⁻¹, and using $H_{ab} = 0.5$ produces a ΔG_{ii}^{\ddagger} of 2.6 kcal mol⁻¹. If, as before, the solvent reorganization contribution is estimated to be 2 kcal mol⁻¹, only 0.6 kcal mol⁻¹ remains for bond reorganization. Consequently, a smaller value of H_{ab} would not be reasonable. Figure 4 also demonstrates that the $\Delta G_{ii}^{\ddagger}(\text{fit})$ values for ferrocenes require smaller H_{ab} values than those for aromatic compounds. If $H'_{ab} = 0.1$ is used for the ferrocenes, as highlighted, their λ_v values are on the order of 16 kcal mol⁻¹ (using λ_s of 8 kcal/mol again) which is significantly larger than λ_v has been argued to be,²³ so an even smaller H_{ab} value might be appropriate.

In contrast to planar aromatics, the $\Delta G_{ii}^{\ddagger}(\text{fit})$ values for Group 1 hydrazines imply a substantial range of H_{ab} values. Double *n*-alkyl replacement of methyl on $\text{Me}_2\text{N}^{0/+}$, going to $\text{nPrMeN}^{0/+}$, $\text{nPr}_2\text{NNMe}_2^{0/+}$, and $\text{nBuMeN}^{0/+}$ raises $\Delta G_{ii}^{\ddagger}(\text{fit})$ by 2.0–2.1 kcal mol⁻¹, and replacing all

four methyls in $\text{Et}_2\text{N}^{0/+}$, $\text{nPr}_2\text{N}^{0/+}$ and $\text{nHx}_2\text{N}^{0/+}$ raises it by 4.1–4.6 kcal mol⁻¹.²⁴ However, λ_v for *n*-alkyl compounds should be no larger than for $\text{Me}_2\text{N}^{0/+}$ (we note that AM1 calculations get ΔH_v to be slightly lower when groups larger than methyl are present; see the last column of Table 1), so their ΔG_{ii}^{\ddagger} values should be the same or slightly lower than that of $\text{Me}_2\text{N}^{0/+}$. Moreover, a slightly smaller λ_s is expected as the alkyl group size increases, yet $\text{Me}_2\text{N}^{0/+}$ is more than >2000 times more reactive than $\text{Et}_2\text{N}^{0/+}$. We believe that H_{ab} may be as large for $\text{Me}_2\text{N}^{0/+}$ as it is for aromatics (ca. 0.5) because of the direct HOMO–LUMO overlap possible, as depicted in Figure 5.

This, in turn, requires that H_{ab} drop to ~ 0.1 for the di-*n*-alkyl compounds and 0.01 for $\text{nR}_2\text{N}^{0/+}$ to account for their lower reactivity in the absence of increased ΔH_v . We suggested that these substantial changes in H_{ab} arise from a steric effect.^{10,11} Nonbonded interactions between *n*-alkyl groups make the methyl groups of $\text{Et}_2\text{N}^{0/+}$ assume alternating positions above and below the nitrogens and α -carbons, which lie nearly in a plane (see Figure 5). This geometry precludes direct overlap of the high-density region of the LUMO near nitrogen of $\text{Et}_2\text{N}^{0/+}$ with the highest density region of the HOMO of Et_2N^0 . In striking contrast, the LUMO of $\text{Me}_2\text{N}^{0/+}$ can achieve significant direct HOMO overlap near nitrogen with an approaching neutral molecule, resulting in a significantly larger H_{ab} . Our data show that no significant increase in $\Delta G_{ii}^{\ddagger}(\text{fit})$ occurs for further enlarging the alkyl groups either by lengthening the alkyl chain or by α -branching. For example, $\text{iPr}_2\text{N}^{0/+}$ has a 0.8 kcal mol⁻¹ lower value than does $\text{Et}_2\text{N}^{0/+}$, which may reflect a lower λ_v .⁹ If “leveling” to a nearly constant H_{ab} did not occur for larger alkyl groups, $\Delta G_{ii}^{\ddagger}(\text{fit})$ s would be unlikely to track calculated λ_v values as they do, since the difference between $\Delta G_{ii}^{\ddagger}(\text{fit})$ and $\lambda/4$ gets larger as H_{ab} decreases, as shown in Figure 2. We examine the postulate that H_{ab} becomes nearly constant for unlinked *n*-alkyl and branched alkyl groups

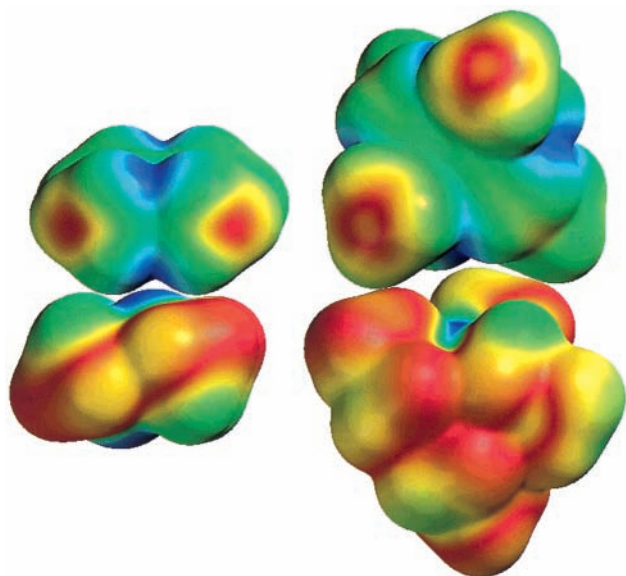


FIGURE 5. HOMO electron density function mapped on the surface density function for $\text{Me}_2\text{N})_2^0$ (lower left) and the LUMO mapped on the surface density function of $\text{Me}_2\text{N})_2^+$ (upper left). Blue indicates the region of highest density for the mapped function; red is zero density. The equivalent functions are displayed for the $\text{Et}_2\text{N})_2^0$ – $\text{Et}_2\text{N})_2^+$ reactant pair on the right. Geometry optimization and electron density function maps were computed at the DFT B3LYP/6-311G* level using Spartan 02.

in Table 1 by showing the ΔG_{ii}^* value calculated by fixing $H_{ab} = 0.01$ for all 13 such compounds. This results in the estimated ΔG_{ii}^* values shown in bold, and a relatively constant ΔG_{ii}^* of 16–17 kcal mol⁻¹ arises for the similar compounds (e.1–4; 7). For Group 1 compounds that do not have four *n*-alkyl groups (i.e., they have some methyl substituents), we calculated H_{ab} values from an assumed ΔG_{ii}^* of 17.0 kcal/mol for *n*-alkyl groups and slightly less for branched alkyl groups and connected the numbers by reverse arrows (←), indicating that H_{ab} is calculated from the assumed ΔG_{ii}^* . This produces intermediate H_{ab} estimates for intermediate numbers of *n*-alkyl groups in agreement with the anticipated steric effects. The N,N-ring compounds $\text{r5NNMe}_2^{0/+}$ and $\text{r6NNMe}_2^{0/+}$ have *n*-alkyl substituents but cannot attain the π -system blocking conformations shown in Figure 5, because the ring restricts alkyl group motion and H_{ab} of 0.45, like $\text{Me}_2\text{N})_2^{0/+}$, is assumed; the more flexible ring system in $\text{r7NNMe}_2^{0/+}$ allows limited alkyl group blocking. This approach produces H_{ab} 's consistent with calculated λ_v 's and that drop substantially when HOMO–LUMO overlap near nitrogen is sterically precluded and ET must proceed through lower-density overlap near alkyl groups. However, it does not appear to drop below about 0.01 for Group 1 hydrazines. The vertical reorganization enthalpies for ET calculated by AM1, shown as ΔH_v , are in remarkably good agreement with the experimental barriers using the $H_{ab} = 0.01$ approximation for Group 3 and 4 hydrazines, too, especially considering how crude these calculations are. Group 2 compounds are expected to have very similar λ_v 's, and a decrease in H_{ab} by a factor of ~ 2 per keto group is necessary to account for the observed increases in ΔG_{ii}^*

(fit) within this group relative to $33\text{N})_2^{0/+}$. This is consistent with a hypothesis that contact for regions near the electron-withdrawing carbonyl groups is ineffective for producing H_{ab} because of low spin density in the radical cations.^{9–11} If the two tetraarylhya-zines studied have about the same ΔG_{ii}^* , the 2.8 kcal mol⁻¹ difference in their ΔG_{ii}^* (fit) values would correspond to a 12-fold smaller H_{ab} value for the hindered $(\text{b}_2\text{P})_2\text{N})_2^{0/+}$, which is consistent with an increase in H_{ab} for replacement of branched alkyl by an unhindered aryl group.

Comparisons with Gas-Phase Reactions. Equation 2 also has been successfully applied to 40 gas-phase ET reactions among some of the hydrazines in acetonitrile that were just described, demonstrating not only that these reactions are activation-limited, but also that solvent reorganization energy is not especially important when vibrational reorganization energy is large.²⁵ The same approach to extracting intrinsic reactivity for gas-phase reactions was used with similar internal agreement. Reactivity was similar to that found in solution with an exception for the reversal of reactivity of [u6]Me₂ and [6]-Me₂, which was attributed to the much higher cation–neutral association energy in the gas-phase precursor complex.

Conclusion

The classical Marcus cross-rate expression, eq 2, correlates all of our data extraordinarily well, implying that these reactions are activation-barrier-limited. These experiments allow accurate estimation of intrinsic reactivity for a wide array of compounds ranging in structure from TMTSF to $\text{nPr}_2\text{N})_2$ and spanning a k_{ij} range of 2×10^{14} . The data set includes many reactions between very hindered compounds that appear limited to transferring an electron via nonbonded contact of saturated alkyl groups. The correlation observed demonstrates that the same intrinsic rate constants suffice whether a couple is reacted with a hydrazine, a ferrocene, or an aromatic compound, and that preexponential factors as well as the barriers for the cross reactions must effectively average. Such behavior is not expected from the perspective of nonadiabatic vibronic coupling ET theory.²¹ Thus, although the effective electronic coupling for electron transfer, H_{ab} , appears to be on the order of only 0.01 for many of the couples studied, their electron transfer cannot be considered “nonadiabatic” in the sense the term is currently used. Although we are unable to make an unequivocal determination of H_{ab} , a combination of rate data, computational results, and available structural data has allowed us to place relatively narrow boundaries on what H_{ab} may be for a wide array of compounds.

We thank the National Science Foundation for partial financial support of this work, currently under grants CHE-9988727(S.F.N.) and CHE-0072928(J.R.P.), and the many students, both undergraduate and graduate, who carried out this work.

References

- (1) See, for example: Lowry, T. H.; Richardson, K. S. *Mechanism and Theory in Organic Chemistry*, 3rd ed.; Harper and Row: New York,

- 1987, for discussion of Hammett Correlations (p 143), solvolysis reactions (p 425), and alkene hydration (p 569).
- (2) (a) Marcus, R. A. On the Theory of Oxidation–Reduction Reactions Involving Electron Transfer. *J. Chem. Phys.* **1956**, *24*, 966–978. (b) Marcus, R. A. Theory of Oxidation–Reduction Reactions Involving Electron Transfer. IV. A Statistical-Mechanical Basis for Treating Contributions from Solvent, Ligands, and Inert Salt. *Discuss. Faraday Soc.* **1960**, *29*, 21–31. (c) Marcus, R. A. On the Theory of Oxidation–Reduction Reactions Involving Electron Transfer. V. Comparison and Properties of Electrochemical and Chemical Rate Constants. *J. Phys. Chem.* **1963**, *67*, 853–857, 2889. (d) Marcus, R. A.; Sutin, N. Electron-Transfer Reactions with Unusual Activation Parameters. A Treatment of Reactions Accompanied by Large Entropy Decreases. *Inorg. Chem.* **1975**, *14*, 213–216.
 - (3) (a) Marcus, R. A.; Sutin, N. Electron Transfer in Chemistry and Biology. *Biochim. Biophys. Acta* **1985**, *811*, 265–322. (b) Sutin, N. Theory of Electron-Transfer Reactions: Insights and Hints. *Prog. Inorg. Chem.* **1983**, *30*, 441–498.
 - (4) Wherland, S. Non-Aqueous, Outer-Sphere ET Kinetics of Transition Metal Complexes. *Coord. Chem. Rev.* **1993**, *123*, 169–99.
 - (5) Ebersson, L. *Electron-Transfer Reactions in Organic Chemistry*; Springer-Verlag: Heidelberg, 1987.
 - (6) Nelsen, S. F.; Wang, Y.; Ramm, M. T.; Accola, M. A.; Pladziewicz, J. R. Ferrocene, Sesquibicyclic Hydrazine Cross-Electron-Transfer Rates. *J. Phys. Chem.* **1992**, *96*, 10654–10658.
 - (7) Nelsen, S. F.; Chen, L.-J.; Ramm, M. T.; Voy, G. T.; Powell, D. R.; Accola, M. A.; Seehafer, T.; Sabelko, J.; and Pladziewicz, J. R. Intermolecular Electron-Transfer Reactions Involving Hydrazines. *J. Org. Chem.* **1996**, *61*, 1405–1412.
 - (8) Nelsen, S. F.; Ismagilov, R. F.; Chen, L.-J.; Brandt, J. L.; Chen, X.; Pladziewicz, J. R. Slow Electron-Transfer Reactions Involving Tetraisopropylhydrazine. *J. Am. Chem. Soc.* **1996**, *118*, 1555–1556.
 - (9) Nelsen, S. F.; Ramm, M. T.; Ismagilov, R. F.; Nagy, M. A.; Trieber, D. A., II.; Powell, D. R.; Chen, X.; Gengler, J. J.; Qu, Q.; Brandt, J. L.; Pladziewicz, J. R. Estimation of Self-Exchange Electron-Transfer Rate Constants for Organic Compounds from Stopped-Flow Studies. *J. Am. Chem. Soc.* **1997**, *119*, 5900–5907.
 - (10) Nelsen, S. F.; Ismagilov, R. F.; Gentile, K. E.; Nagy, M. A.; Tran, H. Q.; Ou, Q.; Halfen, D. T.; Oldegard, A. L.; Pladziewicz, J. R. Indirect Determination of Self-Exchange Electron-Transfer Rate Constants. *J. Am. Chem. Soc.* **1998**, *120*, 8230–8240.
 - (11) Nelsen, S. F.; Trieber, D. A., II.; Nagy, M. A.; Konradsson, A.; Halfen, D. T.; Splan, K. A.; Pladziewicz, J. R. Structural Effects on Intermolecular Electron-Transfer Reactivity. *J. Am. Chem. Soc.* **2000**, *122*, 5940–5946.
 - (12) (a) Nelsen, S. F.; Blackstock, S. C. Measurement of Hydrazine, Hydrazine Radical Cation Self-Exchange Electron-Transfer Rates by ^1H NMR. *J. Am. Chem. Soc.* **1985**, *107*, 7189–7193. (b) Nelsen, S. F.; Kim, Y.; Blackstock, S. C. Solvent Effects on Self-Electron-Transfer Rate Constants for a Sesquibicyclic Hydrazine. *J. Am. Chem. Soc.* **1989**, *111*, 2045–2051.
 - (13) (a) Grampp, G.; Jaenicke, W. Kinetics of Diabatic and Adiabatic Electron Exchange in Organic Systems. Comparison of Theory and Experiment. *Ber. Bunsen-Ges. Phys. Chem.* **1991**, *95*, 904–927. (b) Grampp, G.; Jaenicke, W. ESR–Spectroscopic Investigation of the Homogeneous Electron-Transfer Reactions between Substituted *p*-Phenylenediamines and Quinonediimines, and the Validity of Marcus's Theory. I. Measurements at 293 K. *Ber. Bunsen-Ges. Phys. Chem.* **1984**, *88*, 325–334. (c) Grampp, G.; Jaenicke, W. II. Temperature Dependence and Activation Parameters. *Ber. Bunsen-Ges. Phys. Chem.* **1984**, *88*, 335–340.
 - (14) (a) Nelsen, S. F. Hydrazine, Hydrazine Radical Cation Electron-Transfer Reactions; In *Molecular Structures and Energetics*; Liebman, J. F., Greenberg, A., Eds.; VCH Publishers: Deerfield Beach, FL, 1986; Vol. 3, Chapter 1, pp 1–56. (b) Nelsen, S. F. Hydrazine Stereodynamics; In *Acyclic Organonitrogen Stereodynamics*; Lambert, J. B., Takeuchi, Y., Eds.; VCH: New York, 1992; Chapter 3, p 89–121.
 - (15) (a) Nelsen, S. F.; Peacock, V. E.; Weisman, G. R. Single Electron Oxidation Equilibria of Tetraalkylhydrazines. Comparison of Solution E° Values with Vapor Phase Ionization Potentials. *J. Am. Chem. Soc.* **1976**, *98*, 5269–5277. (b) Nelsen, S. F.; Kessel, C. R.; Brien, D. J. Bredt's Rule Kinetically Stabilized Nitrogen-Centered Radical Cations and Radicals in the 9-Azabicyclo[3.3.1]nonyl System. *J. Am. Chem. Soc.* **1980**, *102*, 702–711. (c) Nelsen, S. F.; Kessel, C. R.; Grezzo, L. A.; Steffek, D. J. Thermodynamic Destabilization of N-Centered Radical Cations by an α -Keto Group. *J. Am. Chem. Soc.* **1980**, *102*, 5482–5485. (d) Nelsen, S. F.; Rumack, D. T.; Meot-Ner(Mautner), M. Gas-Phase Electron-Transfer Equilibrium Studies on Tetraalkylhydrazines: Geometry Effects on Ionization Thermochemistry, Relaxation Energies, and Solvation Energies. *J. Am. Chem. Soc.* **1988**, *110*, 7945–7952. (e) Nelsen, S. F.; Frigo, T. B.; Kim, Y. Sesquibicyclic Hydrazines: Oxidation Thermodynamics and Cation Radical Nitrogen ESR Splitting and UV Absorption Maxima. *J. Am. Chem. Soc.* **1989**, *111*, 5387–5397.
 - (16) (a) Nelsen, S. F.; Hollinsed, W. C.; Kessel, C. R.; Calabrese, J. C. Geometry Change Upon Electron Removal from a Tetraalkylhydrazine. X-ray Crystallographic Structures of 9,9'-Bis-9-Azabicyclo[3.3.1]-nonane and its Radical Cation Hexachlorophosphate. *J. Am. Chem. Soc.* **1978**, *100*, 7876–7881. (b) Nelsen, S. F.; Blackstock, S. C.; Haller, K. J. Oxidation of Molecules Containing Two Hydrazine Units. *Tetrahedron*, **1986**, *42*, 6101–6109. (c) Nelsen, S. F.; Wang, Y.; Powell, D. R.; Hiyashi, R. K. Comparison of Experimental and Calculated Geometries of Sesquibicyclic Hydrazines. *J. Am. Chem. Soc.* **1993**, *115*, 5246–5253. (d) Nelsen, S. F.; Chen, L.-J.; Powell, D. R.; Neugebauer, F. A. 9-Disopropylamino-9-azabicyclo[3.3.1]nonane and Tetraisopropyl Hydrazine Radical Cation: Structure and Conformational Dynamics. *J. Am. Chem. Soc.* **1995**, *117*, 11434–11440. (e) Nelsen, S. F.; Ismagilov, R. F.; Powell, D. R. Charge-localized *p*-Phenylenedihydrazine Radical Cations: ESR and Optical Studies of Intramolecular Electron-Transfer Rates. *J. Am. Chem. Soc.* **1997**, *119*, 10213–10222. (f) Nelsen, S. F.; Tran, H. Q.; Ismagilov, R. F.; Chen, L.-J.; Powell, D. R. Structural Information from Hydrazine Radical Cation Optical Absorption Spectra. *J. Org. Chem.* **1998**, *63*, 2536–2543.
 - (17) Nelsen, S. F. Conformational Studies of Hexahydroimidazole Derivatives. *Acc. Chem. Res.* **1978**, *11*, 14–20.
 - (18) Nelsen, S. F.; Wang, Y. Ring Size and Solvent Effects on Sesquibicyclic Hydrazine Self-Electron-Transfer Rates. *J. Org. Chem.* **1994**, *59*, 1655–1662.
 - (19) Nelsen, S. F.; Frigo, T. B.; Kim, Y.; Blackstock, S. C. Sesquibicyclic Hydrazines: Oxidation Thermodynamics, and Cation Radical Nitrogen ESR Splittings and UV Absorption Maxima. *J. Am. Chem. Soc.* **1989**, *111*, 5387–5397.
 - (20) Selby, T. D.; Blackstock, S. C. Preparation of a Redox-Gradient Dendrimer, Polyamines Designed for One-Way Electron Transfer and Charge Capture. *J. Am. Chem. Soc.* **1998**, *120*, 12155–12156.
 - (21) (a) Bixon, M.; Jortner, J. Electron Transfer—from Isolated Molecules to Biomolecules. *Adv. Chem. Phys.* **1999**, *106*, 35–202 (see p 52). (b) Elliott, C. M.; Derr, D. L.; Matyushov, D. V.; Newton, M. D. Direct Experimental Comparison of Thermal and Optical Electron-Transfer: Studies of a Mixed-Valence Dinuclear Iron Polypyridyl Complex. *J. Am. Chem. Soc.* **1998**, *120*, 11714–11726.
 - (22) Rauhut, G.; Clark, T. Molecular Orbital Studies of Electron-transfer Reactions. *J. Chem. Soc., Faraday Trans.* **1994**, *90*, 1783–1788.
 - (23) McMannis, G. E.; Nielson, R. M.; Gochev, A.; Weaver, M. J. Solvent Dynamical Effects in Electron Transfer: Evaluation of the Electronic Matrix Coupling Elements for Metallocene Self-Exchange Reactions. *J. Am. Chem. Soc.* **1989**, *111*, 5533–5541.
 - (24) The $\Delta G_{if}^{\ddagger}(\text{fit})$ value for $\text{nHx}_2\text{N}_2^{0/+}$ is 0.4 kcal mol $^{-1}$ below that of $\text{Et}_2\text{N}_2^{0/+}$, the largest deviation among these seven compounds. This may be due to a decrease in λ_s expected for increasing molecular diameter. If so, it is much smaller than the 37% smaller λ_s predicted by dielectric continuum theory³ using the volumes of the molecules calculated using AM1.
 - (25) Nelsen, S. F.; Konradsson, A.; Jentzsch, T. L.; O'Konek, J. J.; Pladziewicz, J. R. Comparison of Gas and Solution Phase Intrinsic Rate Constants for Electron Transfer of Tetraalkylhydrazines. *J. Chem. Soc., Perkin Trans. 2* **2001**, 1552–1556.

AR0101077